CHK2 REGULATES MUS81-EME2 FUNCTION IN RESPONSE TO REPLICATION STRESS AND BRCA2 DEFICIENCY

[1 *] Eva Malacaria, [1 *]Anita Palma, [3] Sara Rinalducci, [1] Annapaola Franchitto and [1, 2 §] Pietro Pichierri

* Equally-contributing authors

1 Genome Stability Group, Section of Mechanisms, Biomarkers and Models, Department of Environment and Health, Istituto Superiore di Sanità, Viale Regina Elena 299 - 00161 Rome (Italy)
2 Istituto Nazionale Biofisica e Biostrutture (INBB),Viale delle Medaglie d'Oro, 305 - 00136 Rome (Italy)
3 Proteomics lab, Department of Ecology and Biology, Università della Tuscia, Largo dell'Università - 01100 Viterbo (Italy)

§ Author to whom correspondence should be addressed:

Pietro Pichierri
Tel. +39 0649902994
Fax +39 0660513138
pietro.pichierri@iss.it

ABSTRACT

MUS81 is a structure-specific endonuclease that processes DNA intermediates in mitosis and in S-phase following replication stress. MUS81 is crucial to cleave deprotected reversed forks in BRCA2-deficient cells. However, how MUS81 is regulated during replication stress in human cells remains unknown.

Our study reveals that CHK2 binds the MUS81-EME2 complex and positively regulates formation of DSBs upon replication stress or in the absence of BRCA2. The association with MUS81 occurs through the FHA domain of CHK2 and is disabled by the Li-Fraumeni-associated mutation I157T. The CHK2-MUS81-EME2 complex forms downstream fork reversal and degradation, and phosphorylation of MUS81 at CHK2-targeted sites is crucial to introduce DSBs at deprotected replication forks ensuring the replication fork recovery in BRCA2-deficient cells.

Collectively, our work sheds light into the regulation of the MUS81-EME2 complex and identifies a novel function of the ATM-CHK2 axis in the response to deprotected replication forks in the absence of BRCA2.

INTRODUCTION

The replication stress response is critical for the maintenance of genome integrity and works as an anti-cancer barrier in human cells [1–4]. One of the functions of this response is protection of the replication fork from extensive degradation and collapse [3,5]. To this end, perturbed replication forks are targeted by multiple proteins that coordinate a checkpoint response with fork remodelling and protection in response to sustained arrest [6–8]. One of the critical steps towards fork protection is formation of a reversed fork [8]. Replication fork reversal involves the action of multiple enzymes, including the key activity of SMARCAL1 and the homologous recombination factor RAD51 and BRCA2 [7]. BRCA2 is crucial during homologous recombination to promote RAD51 nucleofilament assembly [9] and is mutated in the majority of familial breast cancers [10,11]. BRCA2 and RAD51 are also required to protect the reversed fork from unscheduled degradation by the MRE11/EXO1 nucleases [7,8]. Loss of BRCA2, indeed, impairs fork protection by RAD51 and stimulates a pathological degradation of nascent strands that eventually results in activation of a recombination-based replication recovery through break-induced replication pathways [12–14].

Pathological degradation and cleavage of reversed forks has been correlated with sensitivity of BRCA2-deficient cells to cisplatin or PARP inhibitors [15–17]. Hence, understanding of this mechanism and its regulation has striking relevance also for cancer therapy. Unfortunately, little is known about the regulation of the pathological fork recovery pathway taking place in the absence of BRCA2.

In BRCA2-deficient cells, one of the critical steps of deprotected fork processing is the cleavage of a flap DNA intermediate by the MUS81-EME2 complex downstream MRE11/EXO1 activity [13,18]. The function of MUS81 in BRCA2-deficient cells is essential to replication fork recovery and to promote viability under conditions of normal or perturbed replication [13,18].

MUS81 is a structure-specific endonuclease that cleaves recombination and replication DNA intermediates generating DSBs. MUS81 forms a heterodimeric complex with Eme1(Mms4) in yeast while human MUS81 can heterodimerize also with EME2 especially in S-phase and to process stalled forks [19]. MUS81-dependent cleavage needs to be tightly regulated during cell cycle to avoid unscheduled DSBs formation in S-phase or insufficient resolution in G2/M [20]. In human cells, the MUS81-EME1 complex activity in G2/M is regulated by CDK1, PLK1 and CK2 [20,21]. In contrast, little is known on how the MUS81 complex is regulated during replication, especially in response to replication stress and in pathological conditions, such as in BRCA2-deficient cells.

In fission yeast, Mus81/Eme1 function is controlled by $Cdc2^{CDK1}$ and Chk1 kinases in response to DNA damage, while the checkpoint kinase $Cds1^{CHK2}$ interacts through its FHA domain with

MUS81 and negatively regulates its function during S-phase in S. pombe [22–25]. In human cells, both CHK1 and CHK2 are activated during replication stress, however, CHK1 is the true functional Cds1 homologue although structurally CHK2 is the homologue of Cds1 [26].

Fork reversal and degradation generate free DNA ends that might activate CHK2 through ATM, in addition to ATR. However, whether CHK2 is involved in the pathological processing of perturbed forks upon replication stress and in the absence of BRCA2 is poorly investigated and is unknown if a functional MUS81-CHK2 crosstalk exists in human cells.

Therefore, in this study, we combined biochemical and single-cell assays to determine if CHK2 controls the formation of MUS81-dependent DSBs at replication forks and whether CHK2 and MUS81 functionally interact upon sustained arrest or loss of BRCA2.

Our study shows that CHK2 and MUS81 physically interact through the FHA domain and that the Li-Fraumeni-related I157T mutation is sufficient to greatly reduce this interaction. Furthermore, we show that CHK2 is involved in regulating formation of MUS81-dependent DSBs when replication forks experience prolonged arrest and when replication forks are destabilised by loss of BRCA2. Finally, we identify residues of MUS81 phosphorylated by CHK2 that are functionally involved in the formation of DSBs at the reversed replication forks in BRCA2-deficient cells.

Our findings identify a crucial regulatory mechanism involved in the control of MUS81-EME2 complex at perturbed replication forks demonstrating that CHK2 activity and binding with MUS81 regulate the cleavage of reversed forks in BRCA2-deficient cells.

RESULTS

MUS81-CHK2 interaction is stimulated by replication stress

To investigate the functional correlation between MUS81 and CHK2 in human cells, we first examined their possible association in a complex by performing immunoprecipitation experiments in HEK 293T cells transiently transfected with GFP-MUS81 and/or HA-CHK2 constructs. Since MUS81 participates in the resolution of DNA intermediates in S-phase during replication stress and in mitosis, we treated cells with hydroxyurea (HU) or nocodazole (NOC) to accumulate cells in S-phase and mitosis, respectively [21]. MUS81 was detected in the anti-HA immunoprecipitates from asynchronous and mitosis-enriched cells, however, HU increased MUS81-CHK2 complex formation 5-fold respect to untreated and 2-fold respect to NOC-treated cells (Fig. 1a). Reciprocal immunoprecipitation with anti-GFP antibodies confirmed the existence of a MUS81-CHK2 complex and its stimulation by replication stress (Fig. 1a). Interestingly and in agreement with the preferential activation of the MUS81/SLX4 complex in mitosis, GFP-MUS81 immunoprecipitated the SLX4 scaffold protein after NOC but barely after HU (Fig. 1a). This result suggests that MUS81 may participate in different complexes when associated with CHK2 or SLX4. Interaction between MUS81 and SLX4 is dependent on phosphorylation at S87 of MUS81 by CK2 and is greatly increased in the S87 phosphomimetic mutant of MUS81 ($MUS81^{S87D}$) [21]. To have further demonstration that MUS81 does not bind to SLX4 when in a complex with CHK2, we transfected HEK 293T cells with HA-CHK2, the wild-type or the S87D form of Flag-MUS81 and performed co-immunoprecipitation experiments (Fig. S1). Consistent with the hypothesis of a nonconcurrent association of MUS81 with CHK2 or SLX4, the S87D mutant showed reduced co-immunoprecipitation with CHK2 in all conditions.

We then investigated the formation of the MUS81-CHK2 complex in shMUS81 MRC5 cells stably complemented with Flag-tagged wild-type MUS81 ($MUS81^{wt}$) where the ectopic MUS81 is expressed at close-to-endogenous levels [21]. CHK2 was detected in anti-Flag-MUS81 immunoprecipitates obtained from $MRC5^{wt}$ cells while it was undetected in anti-Flag immunoprecipitation from the parental shMUS81 cells. Consistent with data from overexpressing cells, replication stress stimulated formation of the endogenous MUS81-CHK2 complex (Fig. 1b). The association between MUS81 and CHK2 was also confirmed at the single-cell level by proximity-ligation assay (PLA). As shown in Figure 1c, MUS81-CHK2 PLA-positive nuclei were detected in untreated $MUS81^{wt}$ cells. Notably, replication stress increased both the number of PLA-positive nuclei and spots. In contrast, PLA signals were undetectable in shMUS81 cells (Fig. 1c).

In human cells, MUS81 can heterodimerize with EME1 or EME2 [27]. EME1 interacts with MUS81 throughout the cell cycle, while binding with EME2 occurs predominantly during S phase [19]. Despite a remarkable increase in the CHK2-MUS81 association after 24h of HU, both EME1 and EME2 were detected in the anti-CHK2 immunoprecipitates (Fig. S2A). Thus, we tested whether the CHK2-MUS81 interaction was affected by depleting each of the two partners of MUS81. Indeed, depletion of each subunit (EME1 or EME2) is expected to disrupt the functionality of only one MUS81 complex. Depletion of EME1 failed to affect MUS81-CHK2 interaction as seen by *in situ* PLA in HU-treated cells, while that of EME2 significantly reduced this association (Fig. S2B), suggesting that the CHK2 preferentially associates with MUS81-EME2 during replication stress.

Having demonstrated that CHK2 forms a complex with MUS81-EME2, we investigated whether this interaction was functional. Prolonged replication fork arrest by HU induces MUS81-dependent cleavage of stalled forks and unresolved replication intermediates [28–30]. Since HU-induced replication stress stimulates MUS81-CHK2 interaction as well as MUS81-dependent cleavage, we next tested if CHK2 kinase stimulated this MUS81-dependent event. To this aim we performed neutral Comet assay in cells treated 24h with HU and the CHK2 inhibitor BML-277 (Fig. 1d). In shMUS81 cells, little DSBs were detected following 24h HU and their number was not affected by inhibition of CHK2 (Fig. 1d). In contrast, accumulated DSBs after 24 hours of HU treatment in MUS81^{wt} cells and their number was significantly reduced by CHK2 inhibition (Fig. 1d). Formation of the MUS81-CHK2 complex correlates with DSBs formation, increasing after HU treatment and showing a strong upregulation at 24 hours as shown comparing parallel PLA and neutral Comet experiments (Fig. S3).

Altogether, these results show that MUS81 and CHK2 form a complex that is stimulated by replication stress and is downregulated in mitosis when MUS81 interacts preferentially with SLX4. Furthermore, our results indicate that CHK2 catalytic activity is required to stimulate MUS81-dependent DSBs formation in response to prolonged replication stress.

The functional interaction with MUS81 involves the FHA domain of CHK2 and is disrupted by the Li-Fraumeni I157T CHK2 mutation

In yeast, Cds1 interacts with Mus81 through its FHA1 protein-docking domain [23]. Thus, we analysed whether, in human cells, the interaction with MUS81 involved the FHA domain of CHK2. As a control, we used a mutant form of the FHA domain of CHK2 containing the Li-Fraumeni syndrome I157T mutation [31] that severely reduces protein interaction but not CHK2 activation [32].

The wild-type and the I157T mutant forms of the human CHK2-FHA domain fused to GST were purified from bacteria and incubated with nuclear extracts from HEK293T cells. We found that the

wild-type FHA domain pulled down efficiently MUS81, while the I157T mutation largely decreased this binding (Fig. 2a). We next performed immunoprecipitation assays in HEK 293T shMUS81 cells co-transfected with FLAG-MUS81 and HA-CHK2^{wt} or HA-CHK2^{I157T}. After 24h of HU, MUS81 was readily detected in anti-HA immunoprecipitates from shMUS81 cells transfected with FLAG-MUS81 but not in the mock-transfected shMUS81 cells (Fig. 2b). However, co-immunoprecipitation between CHK2 and MUS81 was completely abrogated in the presence of the CHK2^{I157T} mutant. Surprisingly, the FHA CHK2^{R117A} mutant, where the substitution of arginine 117 disrupts the phospho-dependent protein binding ability [32], did not affect interaction with MUS81, suggesting that MUS81-CHK2 association does not necessarily involve prior phosphorylation (Fig. 2c).

We show that CHK2 and MUS81 interaction does not take place in mitosis and does not involve SLX4. Consistent with this hypothesis, MUS81 phosphorylation by CK2, including that at S87 required in mitosis (Fig. S4A)[21], abrogates association between MUS81 and the FHA domain of CHK2 in pull-down experiments, confirming that mitotic phosphorylation of MUS81 prevents CHK2 recognition (Fig. S4B).

CHK2 activity apparently sustains MUS81-dependent DSBs after HU treatment (Fig. 1d). Hence, we investigated whether binding of the FHA-CHK2 domain with MUS81 was required to promote DNA breakage upon replication stress. To this aim, we performed neutral Comet assay in MRC5 cells transfected with HA-tagged CHK2^{wt}, CHK2^{I157T} or CHK2^{R117A} (Fig. 2c, d). We reasoned that, since both mutants severely interfere with binding of CHK2 with multiple substrates but association with MUS81 is only abrogated by the Li-Fraumeni-related I157T change, a specific defect in CHK2-MUS81 complex formation would have resulted in suppression of DSBs only in the CHK2^{I157T} mutant. Indeed, CHK2^{I157T} mutant expression abrogates DSBs accumulation after HU-induced replication stress while both CHK2^{wt} or CHK2^{R117A} overexpression failed to affect DSBs formation as compared with control transfected cells (empty) (Fig. 2d).

Altogether, these results demonstrate that formation of the CHK2-MUS81 complex involves the FHA domain of CHK2 and that the association is abrogated by the Li-Fraumeni-related CHK2^{I157T} mutation. Furthermore, our results indicate that disruption of the binding between MUS81 and the CHK2 FHA motif abrogates formation of DSBs under replication stress.

Formation of the MUS81-CHK2 complex and activity of CHK2 promotes DSBs at deprotected forks

The MUS81 complex targets replication forks after their prolonged stalling but also readily cleaves reversed forks in the absence of BRCA2 or other replication caretakers [12,13,29,33–35]. We therefore

investigated if interaction between CHK2 and MUS81 was involved in the generation of DSBs occurring in BRCA2-depleted cells. CHK2 inhibition or CHK2^{I157T} overexpression were used to test the effect of CHK2 activity and MUS81/CHK2 binding on DSBs formation respectively (Fig. 3a, b). As expected, treatment with HU for 2h induced a significant amount of DSBs in absence of BRCA2, as shown by neutral Comet assay. Exposure of cells to the BML-277 CHK2 inhibitor before and during HU treatment greatly reduced formation of DSBs. Similarly, overexpression of the dominant-negative FHA I157T CHK2 mutant reduced the formation of DSBs almost completely. Of note, in BRCA2-depleted cells, expression of the CHK2^{I157T} mutant or the absence of MUS81 each reduced DSBs although expression of the CHK2^{I157T} mutant appeared slightly more efficient in preventing DSBs (Fig S5A). Moreover, inhibition of ATM, the apical CHK2 kinase, strongly reduced formation of DSBs in BRCA2-depleted cells after treatment with HU (Fig. S5B).

Consistent with a role of CHK2 in modulating the function of the MUS81 complex at deprotected forks, its activatory phosphorylation at T68 and that of ATM at S1981 were both elevated in the absence of BRCA2, especially at 2h of treatment (Fig. S6A). To further investigate if the increased activation of the ATM-CHK2 axis observed in BRCA2-depleted cells originated from stalled replication forks, we analysed recruitment of active ATM at nascent DNA by SIRF using anti-pS1981ATM antibodies (Fig. 3c). We expected that more active ATM should be recruited early to replication forks in absence of BRCA2. Interestingly, active ATM was found associated with replication forks already at 2h also in BRCA2-proficient cells and its fork association increased at 4h of HU to decline thereafter. However, more pS1981 ATM was detected at stalled forks in the absence of BRCA2 and the fraction of fork-associated pS1981ATM remained constant also at later time-points. Of note, analysis of formation of pS1981ATM nuclear foci in chromatin fractionated cells after MUS81 depletion indicated that elevated ATM activation in cells depleted of BRCA2 occurs independently of the MUS81-dependent formation of DSBs (Fig. S6B).

We therefore concluded that activation of CHK2 and its interaction with MUS81 are required for early DSBs formation occurring in BRCA2-depleted cells. Thus, we wanted to determine if the interaction between CHK2 and MUS81 was stimulated by the absence of BRCA2. Hence, we performed PLA experiments in cells exposed to HU for different time-points. Surprisingly, a substantial CHK2-MUS81 interaction was detected 2h after replication arrest in siCTRL transfected cells (wild-type, BRCA2-proficient, cells) and persisted at 4h (Fig. 4a), suggesting that CHK2 and MUS81 form a complex also when MUS81 does not target perturbed replication forks. Cells depleted of BRCA2 (siBRCA2) showed a significant increase in the number of CHK2-MUS81 PLA spots at 2h of HU but a decline to wild-type levels at 4h (Fig. 4a). Combined PLA and EdU

detection confirmed that, in BRCA2-deficient cells, the majority of PLA spots occurred in S-phase, consistent with the CHK2-MUS81 interaction taking place during replication arrest (Fig. S7).

To determine whether formation of the CHK2-MUS81 complex occurred downstream fork reversal in BRCA2-deficient cells, we performed PLA in cells depleted of SMARCAL1, one of the crucial enzymes involved in this pathway [36].

As expected, a number of CHK2-MUS81 PLA spots was detected already in cells transfected with siCTRL (BRCA2-proficient) after replication arrest (Fig. 4b). Transfection with siBRCA2 oligos stimulated formation of a CHK2-MUS81 complex in response to perturbed replication and concomitant depletion of SMARCAL1 greatly reduced the interaction of MUS81 with CHK2 at both time-points (Fig. 4b). However, depletion of SMARCAL1 did not suppress interaction between MUS81 and CHK2 completely in cells depleted of BRCA2. As multiple enzymes contribute to fork remodelling, we performed PLA experiments in cells pre-treated with Olaparib, a condition that prevents fork reversal [37]. As expected, depletion of BRCA2 led to elevated levels of CHK2-MUS81 PLA spots already at 2h of HU treatment, which were almost completely absent in cells pre-treated with Olaparib (Fig. 4c).

In BRCA2-depleted cells, MUS81 functions downstream degradation of reversed forks mediated by MRE11 and in a RAD52-dependent manner [13,14,38,39]. Thus, to determine the mechanism underlying formation of the CHK2-MUS81 complex, we performed PLA experiments in BRCA2-depleted cells in which MRE11 was inhibited with Mirin or RAD52 with EGC (RAD52i; [38]). Again, multiple PLA spots were observed in BRCA2-depleted cells after HU treatment indicative of the CHK2-MUS81 interaction, and, interestingly, either Mirin or the RAD52i completely suppressed formation of PLA spots (Fig. 4d).

Collectively, these results indicate that the ATM-CHK2 axis is activated to promote MUS81-dependent DSBs in BRCA2-depleted cells and that the formation of the MUS81-CHK2 complex occurs downstream fork reversal and after fork degradation by MRE11.

The MUS81-CHK2 complex and CHK2 activity contribute to fork recovery in absence of BRCA2

In BRCA2-deficient cells, MUS81 activity is required for regressed fork cleavage and subsequent replication restart [13]. Thus, we analysed whether inhibition of CHK2 or mutation of its FHA domain to abrogate the interaction with MUS81 could affect recovery from replication arrest in BRCA2-depleted cells. To this end, we treated BRCA2-depleted cells with CHK2i or transfected them with the I157T or R117A FHA-CHK2 mutant, which disables or not the CHK2-MUS81 interaction respectively (Fig. 5a). Replication fork recovery was evaluated as the residual number of stalled

forks on stretched DNA fibres prepared from cells pulse labelled with CldU and IdU (Fig. 5b). Consistent with previous data [13], replication fork recovery was reduced in cells depleted of BRCA2 and was largely dependent on MUS81. Inhibition of CHK2 in BRCA2-depleted cells also increased the number of stalled forks after recovery from HU treatment and, notably, phenocopied MUS81 depletion (Fig. 5b). Interestingly, the residual number of stalled forks was similarly increased by expression of the I157T FHA-CHK2 mutant, which compromised MUS81 binding, while was not affected by the R117A FHA-CHK2 mutant that retains normal MUS81 binding.

Inability of MUS81 to cleave resected reversed forks increases the number of intact reversed forks in BRCA2-deficient cells and this contributes to inability to properly resume replication [13]. We previously showed that ectopically expressed bacterial RuvA, an avid binder of HJs, accumulates in chromatin under conditions stimulating formation of reversed forks [39]. Thus, we used this endpoint as a proxy of the presence of reversed forks in cells stably-expressing a dox-regulated shBRCA2 cassette and transfected transiently with the CHK2 mutants, alone or in combination with siMUS81 oligos (Fig. 5c, d).

As shown in Figure 5d, HU treatment induced the presence of chromatin-associated RuvA in the absence of DOX (WT cells), consistent with the presence of HJ-like structures, including reversed forks. Depletion of BRCA2 by DOX treatment, slightly reduced the presence of RuvA in chromatin, which was increased by concomitant depletion of MUS81, as expected if chromatin-bound RuvA marks reversed forks that persist if left uncleaved (Fig. 5c). Interestingly, expression of the $CHK2^{I157T}$ mutant, which does not bind MUS81, also greatly increased the amount of RuvA in chromatin in BRCA2-depleted cells but did not further increase the presence of RuvA if combined to MUS81 depletion.

Nascent ssDNA is formed as the result of resected reversed forks [13,39–41]. CHK2 inhibition or inability to interact with MUS81 did not significantly decrease the amount of exposed nascent ssDNA (Fig S8) in agreement with the function of MUS81 downstream fork degradation by MRE11-EXO1 [13].

These results indicate that the interaction of CHK2 with MUS81 is required for the recovery of the stalled forks in the absence of BRCA2, possibly stimulating correct targeting of reversed forks downstream fork degradation.

CHK2-dependent phosphorylation of MUS81 at S97 controls formation of DSBs under replication stress

FHA domain mediates the recognition of CHK2 substrates [42]. To test if MUS81 is a CHK2 substrate, we performed an *in vitro* phosphorylation assay. As substrate we used the 76-206 N-terminal region of human MUS81 that contains an essentially unstructured region including SLX4 binding residues [43,44] and several putative phosphorylation sites [21]. The purified N-terminal fragment of MUS81 fused to GST was incubated with recombinant CHK2 kinase, subjected to SDS-PAGE and analysed by MS/MS (Fig. 6a). Mass spectrometry identified two major phosphorylation sites, Thr 86 and Ser 97, in the MUS81 fragment *in vitro* (Table 1 and Figures S9 and S10). To determine if MUS81 phosphorylation at S97 had any functional relevance in response to replication stress, we performed neutral Comet assay in shMUS81 cells transiently transfected with wild-type MUS81 or its unphosphorylable (T86A, S97A) or phosphomimetic (T86D, S97D) mutants. Strikingly, the putative CHK2 unphosphorylable T86A and S97A MUS81 mutants were both unable to support HU-induced DSBs accumulation and combined CHK2 inhibition did not further reduce DSBs, supporting that phosphorylation of those sites depends on CHK2 also in the cell. The phosphomimetic T86D MUS81 mutant showed a wild-type ability to induce DSBs after prolonged HU treatment but not in untreated conditions, while the S97D MUS81 mutant caused a striking amount of DSBs formation already under unchallenged replication.

We next investigated whether MUS81-S97A and S97D were able to affect DSBs formation also at deprotected forks. We focused on S97 because the phenotype of the phosphomimetic S97D mutation suggested that it could represent an event involved under pathological replication and needing to be strictly controlled. To this end, we performed neutral Comet assay upon depletion of BRCA2 and transient transfection of the unphosphorylable or phosphomimetic MUS81 mutants (Fig. 6c). As reported previously[13,29], a short treatment with HU failed to induce any detectable DSBs in wild-type cells (Fig. 6c). Of note, $MUS81^{S97A}$ was unable to support DSBs formation in siBRCA2-transfected cells. Expression of $MUS81^{S97D}$ strongly enhanced the amount of DSBs even after a 2h treatment with HU in siCTRL-transfected, BRCA2-proficient, cells. Interestingly, expression of $MUS81^{S97D}$ in BRCA2-depleted cells did not increase further the level of DNA breakage respect to BRCA2-proficient cells (siCTRL), possibly suggesting that phosphorylation on this residue needs to be maintained elevated under this condition.

Neutral Comet assay suggests that S97 of MUS81 needs to be phosphorylated by CHK2 in BRCA2-depleted cells. Since, in these conditions, DSBs are required for the recovery of stalled replication forks (Fig. 5b), we quantified the percentage of replication forks stalling by DNA fiber assay after HU treatment. To this end, we used $MUS81^{KO}$ cells stably-expressing a dox-regulated shBRCA2 cassette and transfected transiently with the S97 CHK2 mutants (shBRCA2 $MUS81^{KO}$ ([45]; Fig 6d)

Although the number of stalled forks is low after 2h of HU, the fraction of stalled forks in BRCA2-depleted cells increased significantly after expression of MUS81^{S97A}, phenocopying what was observed after CHK2 inhibition (see Fig 5b). Interestingly, inhibition of CHK2 in BRCA2-depleted cells expressing MUS81^{S97A} failed to further increase the number of stalled forks. In addition to impinge on the number of stalled forks restarting DNA synthesis, expression of the MUS81^{S97A} in BRCA2-depleted cells also affected the efficiency of fork restart reducing the length of IdU tracts (Fig. 6e).

These results indicate that CHK2 can target MUS81 at multiple residues and that phosphorylation status of these residues is critical to regulate the formation of MUS81-dependent DSBs and to promote restart of stalled replication forks in BRCA2-depleted cells.

CHK2-MUS81 interaction promotes survival of BRCA2-deficient cells upon replication stress.

MUS81 cleaves intact forks and partially regressed forks in wild-type cells or BRCA2-depleted cells, respectively [13,28], leading to rescue after genotoxic stress or replication fork deprotection. To test whether loss of CHK2-MUS81 complex formation was required for survival of BRCA2-deficient cells after HU treatment, we quantified the viability of cells after transient expression of the wild-type form of CHK2 or the CHK2^{I157T} mutant disabling the interaction of the FHA domain with MUS81. We used MUS81^{KO} cells stably-expressing a dox-regulated shBRCA2 cassette (in brief, MUS81^{KO}) or their non-edited counterpart expressing wild-type MUS81 [45]. As reported by others [13], concomitant loss of BRCA2 and MUS81 sensitized cells to HU treatment (Fig. 7a). Expression of the CHK2^{I157T} mutant increased HU sensitivity in BRCA2-depleted cells also in the presence of the wild-type form of MUS81 as compared with cells expressing CHK2^{wt} (Fig. 7a). Interestingly, expression of the CHK2^{I157T} mutant did not strikingly enhance sensitivity to HU in MUS81^{KO}, BRCA2-depleted, cells (Fig. 7a).

Thus, either MUS81 KO or abrogation of the interaction with CHK2 is sufficient to induce a similar hypersensitivity to HU in BRCA2-depleted cells.

DISCUSSION

In this work, we have shown that activation of the MUS81-EME2 complex during prolonged replication fork arrest or pathological responses to fork stalling requires activity of CHK2 and its association with MUS81 through the FHA domain. CHK2 activity, binding to and phosphorylation of MUS81 are critical events for the processing of reversed forks into DSBs when BRCA2 is absent, contributing to replication fork recovery and viability (Fig. 7b). This defines a previously unappreciated regulatory mechanism of the MUS81-EME2 complex during replication fork cleavage and restart upon replication stress and deprotection of reversed forks.

Since formation of DSBs at the replication fork can lead to gross chromosomal rearrangements, activity of the MUS81 endonuclease is normally blocked or negatively-regulated in S-phase [27]. In yeast, the Mus81 complex is inhibited during normal replication or following transient arrest by Cds1, while checkpoint kinases stimulate its function, cooperating with Cdks, in response to DNA damage in S-phase or, in budding yeast, when Rqh1 is absent [22,24,25,46,47].

In human cells, phosphorylation of EME1 by CDK1/PLK1 and of MUS81 by CK2 on Serine 87 restrict the activation of SLX4-MUS81-EME1 complex in late G2/M, preventing aberrant cleavage in S-phase [21,48]. Here, we find that HU-induced replication stress leads to the formation of a CHK2-MUS81 complex. Notably, CHK2 preferentially recognizes MUS81 when complexed with EME2 instead of EME1, consistent with previous work showing EME2 relevance in S-phase [19,30,49]. Although depletion of SLX4 was reported to abrogate DSBs upon replication arrest [50], we failed to detect SLX4 when MUS81 and CHK2 are co-immunoprecipitated from S-phase cells. Moreover, CHK2 does not bind a MUS81 mutant mimicking constitutive mitotic phosphorylation by CK2 and consequently promoting association with SLX4 [21]. Thus, the CHK2-MUS81-EME2 complex is clearly stimulated upon replication stress but apparently misses SLX4. These data suggest for the existence of different nuclease complexes in S-phase or M-phase. However, previous data from our group and others implicated MUS81/EME1 in the response to CHK1 inhibition or oncogene-induced replication stress [33–35] indicating that different and specific complexes of MUS81 might form also in S-phase under pathological conditions.

In yeast, the inhibitory interaction between Cds1 and MUS81 involves the FHA domain of Cds1 [23,24]. Our data clearly indicate that the CHK2-FHA domain is responsible for MUS81 binding also in humans, although we find that CHK2 regulates positively MUS81-dependent DSBs formation after replication stress. Although binding of Cds1 to Mus81 is phosphodependent [24], we failed to identify a phosphorylation-dependent CHK2-FHA-MUS81 interaction. However, FHA domains show versatile and broad specificity, binding canonical phosphopeptides as well as non-canonical

and non-phosphorylated sequences [51,52], possibly suggesting that the CHK2-MUS81 association involves a FHA-mediated but phospho-independent interaction occurring in a distinct FHA peptide-binding surface [32,42]. Interestingly, we find that the Li-Fraumeni syndrome-associated FHA ^{I157T} mutation largely impairs MUS81-CHK2 interaction and MUS81-dependent DSBs under replication stress. In contrast, but consistent with a phospho-independent interaction, the FHA^{R117A} mutant, which impairs the affinity for target phosphates and abolishes CHK2 interaction with BRCA1 [32], does not affect MUS81 binding and function in response to replication stress.

The MUS81/EME2 complex is crucial also to overcome fork deprotection induced by loss of BRCA2 [13]. However, it is also crucial that MUS81/EME2 targets only degraded replication forks. Our findings reveal that CHK2-dependent regulation of MUS81 is required for DSBs formation and fork restart in BRCA2-deficient cells. Interestingly, association between CHK2 and MUS81 is stimulated in BRCA2-deficient cells and CHK2 or ATM activatory phosphorylation at T68 or S1981, respectively, are elevated in the absence of BRCA2 early after replication arrest. Moreover, phosphorylated ATM can be detected at stalled forks independently of the presence of MUS81. These results suggest that ATM-CHK2 is activated prior to DSBs formation in BRCA2-deficient cells, consistent with an upstream role in regulating MUS81/EME2 function. Interestingly, active, S1981-phosphorylated, ATM can be detected at stalled replication forks even in BRCA2-proficient cells where DSBs are undetectable. This last observation is consistent with the recognition of DNA ends of reversed forks by DSB binding factor, like KU [53]. Indeed, MUS81-CHK2 PLA spots can be detected also in BRCA2-proficient cells. This indicates that the MUS81-CHK2 complex is assembled whenever forks get stalled but is kept inactive or that a fraction of stalled forks are unstable even in the presence of BRCA2, stimulating assembly of the complex. Further studies will be required to discriminate between these two hypotheses. Formation of the MUS81-CHK2 interaction is greatly reduced when fork reversal is impaired. Consistent with this, preventing MRE11 from binding to or degrading the reversed fork interferes with MUS81-CHK2 interaction in the absence of BRCA2.

Upon loss of BRCA2, MUS81 acts downstream CtIP, MRE11 and EXO1 nucleases to mediate cleavage of a flapped DNA at the reversed forks [13]. Thus, our data indicate that the MUS81-CHK2 complex is assembled downstream fork remodelling to ensure that cleavage occurs only at specific DNA intermediates.

In absence of MUS81-dependent cleavage, extensively resected forks cannot properly restart [13]. Consistent with this, loss of CHK2-dependent MUS81 regulation conferred by the FHA I157T mutation impairs cleavage of stalled replication forks with their significant accumulation and severe consequences on the ability to restart replication and overcome replication stress.

Mutations of ATM or CHK2 predispose to breast cancer and the ATM-CHK2 pathway has been shown to support MUS81 activity to generate DSBs in response to cisplatin treatment in a human breast cancer model [54]. In addition, the missense CHK2 I157T mutation associated to Li-Fraumeni syndrome [31,55], is linked with breast cancer (odds ratio = 1.4) and increases the risk of breast cancer if carriers already have deleterious mutations of CHK2 and BRCA1/2 [56]. Thus, inability to properly regulate MUS81-EME2 at distressed forks might contribute to susceptibility to cancer development. Of note, CHK2 can target at least two distinct MUS81 residues, *in vitro*. Mutations abrogating phosphorylation at these two residues suppress MUS81-dependent DSBs after prolonged replication arrest in wild-type cells suggesting that modification of these sites is functional. Interestingly, the two putative CHK2 phosphorylation sites localise close to the N-terminal region of MUS81 involved in the interaction with SLX4 that acts to relieve the auto-inhibitory binding between the Hairpin-helix-hairpin domain of MUS81 and the EME1 subunit [44]. Given the ample structural similarities between EME1 and 2 [57], it is tempting to speculate that phosphorylation by CHK2 might promote a conformational change similar to that induced by interaction with SLX4 thus leading to an active MUS81-EME2 complex. Inability of S>A MUS81 mutants to induce DSBs and elevated DSBs in the S97D mutant, even in untreated conditions, may be consistent with the presence of an inactive CHK2-MUS81 complex requiring regulated phosphorylation for its full activation.

In conclusion, this work sheds light on regulation of the MUS81/EME2 complex and identifies how CHK2 regulates the response of BRCA2-deficient cells to deprotected forks. Since activation of MUS81 at deprotected forks has been correlated with response to Olaparib [15,16] and inactivating CHK2 mutations can be found in breast cancer and Li-Fraumeni syndrome predisposing to breast cancer [58,59], our work might be of value for the identification of novel biomarkers of PARPi resistance. For instance, our work predicts that Li-Fraumeni patients with the CHK2 mutation are poor responders to Olaparib but possibly sensitive to gemcitabine, which induces replication arrest similar to HU.

In addition, because CHK2 inhibitors are being evaluated in preclinical studies, our mechanistic evidence may be helpful for an educated combination of DDR inhibitors to avoid “self-inactivating” combinations of inhibitors.

ACKNOWLEDGMENTS

We are grateful to Drs Domenico Delia and Giacomo Buscemi for the gift of the pcDNA3-HA-Chk2 plasmid. We are grateful to Prof. Massimo Lopes for scientific discussion. This work was supported by the Italian Ministry of Health “Ricerca Finalizzata” to P.P. (grant n. RF-2016-

02362022) and by investigator grants from Associazione Italiana per la Ricerca sul Cancro (AIRC) to P.P. (IG n. 21428) and to A.F. (IG n. 19971).

AUTHOR CONTRIBUTIONS

A.P. performed all the biochemical experiments and functional characterisation of the MUS81-CHK2 complex formation. E.M. performed the analysis of fork recruitment in vivo, analysis of ATM-CHK2 activation, analysis of RuvA chromatin recruitment, DNA fibers assays and most of the functional analysis of the MUS81 phosphorylation mutants. S.R. performed the analysis of MUS81 phosphorylation and MS to identify phosphorylated residues. A.P., E.M., S.R., analysed data and contributed to designing the experiments and writing the paper. A.F. and P.P designed experiments, analysed data, supervised research and wrote the paper. All authors approved the paper. E.M. and A.P. contributed equally to this work and should be regarded as joint first authors.

COMPETING INTEREST

The authors declare that they do not have any conflict of interest.

MATERIALS AND METHODS

Cell lines and culture conditions

The MRC5SV40 cells were maintained in Dulbecco's modified Eagle's medium (DMEM; Life Technologies) supplemented with 10% foetal bovine serum (Boehringer Mannheim) and incubated at 37 °C in a humidified 5% CO2 atmosphere. Stable shMUS81 MRC5SV40 were described in Palma et al [21]. The wild type form of RNAi-resistant MUS81 ORF cloned into the pEF1a-IRES-NEO plasmid was subjected to SDM (Quickchange II XL – Stratagene) to introduce the T86 or S97 mutations. Sequence-verified plasmids were then transfected into MRC5 shMUS81 cells by the Neon nucleofector (Life technologies). To generate shBRCA2 inducible cell lines, MRC5SV40 were transduced with lentivirus expressing an shBRCA2 cassette under the control of a Dox-regulated promoter at 0.5 of multiplicity of infection (MOI) (Dharmacon SmartVector inducible lentivirus, sequence code V3SH7669-225202141; [45]). After puromycin selection at 300 ng/ml, a single clone was selected and used throughout the study.

Transfections

RNA interference against MUS81 was performed using FlexiTube HsMUS81 6 (Qiagen) at final concentration of 10 nM using Lullaby 48 h before to perform experiments. BRCA2 was depleted with ON-TARGETplus Human BRCA2-SMARTpool (Dharmacon) at 25 nM using Interferin (Polyplus) and experiments were performed after 48 h of transfection. RNA interference against EME2 was performed with SMARTPOOL siRNA della Dharmacon (geneID 197342). The efficiency of protein depletion was monitored by western blotting 72 h after transfection. MRC5, MRC5 shMUS81/MRC5 shMUS81 S87D or shMUS81 S97A cell lines were transfected with pcDNA3-HA-Chk2 (wild-type or with CHK2 mutation) using Neon transfection system 48 h prior to perform experiments.

Chemicals

HU was added to culture medium at 2 mM from stock solutions 200 mM prepared in Phosphate-buffer saline solution (PBS) to induce DNA replication arrest or DNA damage. MIRIN, the inhibitor of MRE11 exonuclease activity (Calbiochem), was added to DMEM 15 min prior HU at 50 µM. Nocodazole (Sigma-Aldrich) was used at 0.5 µg/µl. The BML-277 CHK2 inhibitor (Calbiochem) was used at 10 µM. CldU (Sigma-Aldrich) was dissolved in sterile water at 200mM stock solution and used at 50 µM. IdU (Sigma-Aldrich) was dissolved in sterile DMEM as a stock

solution 2.5 mM and stored at −20 °C. RAD52 inhibitor, EGC (Sigma-Aldrich) was dissolved in DMSO at 100 mM, and stock solution was stored at - 80 °C and was used at 50 µM.

Phosphorylation site prediction

For the prediction of MUS81 phosphorylation sites, the MUS81 protein sequence was scanned using the GPS 2.0 software (http://gps.biocuckoo.org/download.php) with a medium threshold that consist in a < 6% of false identification rate [60]

Production and purification of GST-fused fragments

The FHA domain of CHK2 was amplified by PCR from the pcDNA3-HA-CHK2 plasmid containing the full-length wild-type or mutant CHK2 ORF (a gift from Dr. Domenico Delia's lab). PCR-amplified DNA was cloned into the GST-pGEX-2TK plasmid (Stratagene). GST-FHA fragment was expressed into E.coli BL21PlysS at 30°C for 4h. Bacterial pellets were lysed in BER reagent (Pierce) supplemented with DNase and Lysozyme, as indicated by the manufacturer, and purified by incubation with GSH-magnetic beads (Promega) after extensive washings, as reported previously [61]. Quantification of the magnetic-beads-bound fragments was performed after SDS-PAGE and Coomassie staining against serial dilutions of purified BSA. Magnetic beads-bound GST-FHA fragments were then used as substrates for pull-down assays.

Western blot analysis

Blots were incubated with primary antibodies against: anti-MUS81 (Santa Cruz Biotechnology, 1:2000), anti-Lamin B1 (Abcam, 1:20000), anti-CHK2 (Santa Cruz Biotechnology, 1:1000), anti-BRCA2 (Bethyl, 1:2000), anti-pCHK2 (Millipore, 1:2000), anti-SMARCAL1 (Bethyl, 1:2000), anti-GFP (Santa Cruz Biotechnology, 1:1000), anti-pS1981ATM (Cell signaling, 1:1000), anti-ATM (Cell signaling, 1:1000), anti-HA (Cell signaling, 1:1000), anti-Cyclin A (Santa Cruz Biotechnology, 1:1000), anti-SLX4 (Novus Biologicals, 1:2000), anti-EME1 (Santa Cruz Biotechnology, 1:500), anti-EME2 (Thermo Fisher, 1:1000), anti-FLAG (Sigma Aldrich, 1:2000). After incubations with horseradish peroxidase-linked secondary antibodies (Jackson ImmunoResearch, 1:30,000), the blots were developed using the chemiluminescence detection kit ECL-Plus (Amersham) according to the manufacturer's instructions. Quantification was performed on blot acquired by ChemiDoc XRS+ (Bio-Rad) using Image Lab software, and values shown on the graphs represent a normalisation of the protein content evaluated through Lamin B1 or GAPDH immunoblotting. A complete list of antibodies and dilutions is provided in Supplementary Table 2.

Immunofluorescence

Cells were grown on 35-mm coverslips and harvested at the indicated times after treatments. For immunofluorescence (IF), after further washing with PBS, cells were pre-extracted with 0.5% Triton X-100 and fixed with 3% para-formaldehyde (PFA)/2% sucrose at room temperature (RT) for 10 min. After blocking in 3% bovine serum albumin (BSA) for 15 min, staining was performed with mouse monoclonal anti-phospho-ATM Ser1981 (Millipore 1:300) diluted in a 1% BSA/0.1% saponin in PBS solution, for 1 h at 37 °C in a humidifier chamber. After extensive washing with PBS, Alexa Fluor® 488 conjugated-goat anti-mouse was used at 1:200 and applied for 1 h at RT followed by counterstaining with 0.5 mg/ml 4,6-diamidino-2-phenylindole (DAPI).

Detection of ssDNA by native IdU assay

To detect nascent ssDNA cells were labelled with 80 μM IdU for 20 min before treatments. Untreated cells were labelled for 20 min prior to performing immunofluorescence. For IdU detection cells were subjected to extensive washing with PBS , permeabilized with 0,5% TRITON-X 100 at 4° for 8 min and then fixed with 3% PFA/ 2% Sucrose. Fixed cells were blocked with 3% BSA for 20 min and incubated with primary antibody anti-IdU antibody (Becton Dickinson 1:100) for 1 h at 37 °C in 1% BSA/PBS in a humid chamber, followed by species-specific fluorescein-conjugated secondary antibody Alexa Fluor 488 (Goat Anti-Mouse IgG (H + L), highly cross-adsorbed—Life Technologies) diluted 1:200 in 1% BSA/PBS for 1 h at room temperature . After extensive washing with PBS, cells were stained with 0.5 mg/ml 4,6-diamidino-2-phenylindole (DAPI). Slides were analysed with Eclipse 80i Nikon Fluorescence Microscope, equipped with a Video Confocal (ViCo) system. For each time point, at least 100 nuclei were examined by two independent investigators and foci were scored at 40×. Quantification was carried out using the ImageJ software.

In situ PLA assay for protein–protein interaction

The in situ PLA (DuoLink, Merck) was performed according to the manufacturer's instructions. After indicated treatments, cells were permeabilized with 0.5% Triton X-100 for 10 min at 4 °C, fixed with 3% PFA/2% Sucrose solution for 10 min and then blocked in 3% BSA/PBS for 15 min. After washing with PBS, cells were incubated with the two relevant primary antibodies. The primary antibodies used were as follows: mouse monoclonal anti-FLAG (SIGMA 1:100),rabbit polyclonal anti-CHK2 (Santa Cruz, 1:70). Samples were incubated with secondary antibodies conjugated with PLA probes MINUS and PLUS: the PLA probe anti-mouse PLUS and anti-rabbit MINUS. The incubation with all antibodies was accomplished in a humidified chamber for 1 h at

37 °C. Next, the PLA probes MINUS and PLUS were ligated using two connecting oligonucleotides to produce a template for rolling-circle amplification. After amplification, the products were hybridised with red fluorescence-labelled oligonucleotide. Samples were mounted in Prolong Gold anti-fade reagent with DAPI (blue). Images were acquired randomly using Eclipse 80i Nikon Fluorescence Microscope, equipped with a Video Confocal (ViCo) system.

Quantitative in situ analysis of protein interactions at DNA replication forks (SIRF assay)

10.000 cells were plated onto chamber slides the day before the experiment. The day of experiment, cells were incubated with 125 µM EdU for 8 min, followed 2mM HU as indicated. After treatments, cells were fixed with 2% PFA/PBS for 15 min at RT. Cells were permeabilized in 0,25% Triton X-100 in PBS for 15 min at room temperature. Click reaction cocktail was added into slides (30 µl/well) and incubated at room temperature 30 min in a humid chamber protected from light. Slides were washed with PBS and blocked in 3% BSA/PBS for 20 min. After washing with PBS, cells were incubated with the primary antibodies. The primary antibodies used were rabbit polyclonal anti- Biotin (Abcam 1:500) and mouse monoclonal anti-phospho-ATM Ser1981 (Millipore 1:300). Samples were incubated with secondary antibodies conjugated with PLA probes MINUS and PLUS: the PLA probe anti-mouse PLUS and anti-rabbit MINUS (OLINK Bioscience). The incubation with all antibodies was accomplished in a humidified chamber for 1 h at 37 °C. Next, the PLA probes MINUS and PLUS were ligated using two connecting oligonucleotides to produce a template for rolling-circle amplification. After amplification, the products were hybridised with red fluorescence-labelled oligonucleotide. Samples were mounted in Prolong Gold anti-fade reagent with DAPI (blue). Images were acquired randomly using Eclipse 80i Nikon Fluorescence Microscope, equipped with a Video Confocal (ViCo) system.

DNA Fiber assay

Cells were pulse-labelled with 50 µM CldU for 20 min, washed twice with PBS and treated with HU 2mM as reported in the experimental schemes. After treatments cells were washed twice with PBS and incubated for 40 min in fresh medium with 250 µM IdU. DNA fibres were prepared and analysed to evaluate fork restart [39]. For immunodetection of labelled tracks, the following primary antibodies were used: rat anti-CldU/BrdU (Abcam) and mouse anti-IdU/BrdU (Becton Dickinson).

Chromatin isolation

Cells (4 × 10 × 6 cells/ml) were resuspended in buffer A (10 mM HEPES, [pH 7.9], 10 mM KCl, 1.5 mM MgCl2, 0.34 M sucrose, 10% glycerol, 1 mM DTT, 50 mM sodium fluoride, protease

inhibitors [Roche]). Triton X-100 (0.1%) was added, and the cells were incubated for 5 min on ice. Nuclei were collected in pellet by low-speed centrifugation (4 min, 1300 × *g*, 4 °C) and washed once in buffer A. Nuclei were then lysed in buffer B (3 mM EDTA, 0.2 mM EGTA, 1 mM DTT, protease inhibitors). Insoluble chromatin was collected by centrifugation (4 min, 1700 × *g*, 4 °C), washed once in buffer B + 50 mM NaCl, and centrifuged again under the same conditions. The final chromatin pellet was resuspended in 2X Laemmli buffer and sonicated for 15 s in a Tekmar CV26 sonicator using a microtip at 25% amplitude.

Neutral comet assay

DNA breakage induction was evaluated by Comet assay (single-cell gel electrophoresis) in non-denaturing conditions. Briefly, dust-free frosted-end microscope slides were kept in methanol overnight to remove fatty residues. Slides were then dipped into molten low melting point (LMP) agarose at 0.5% and left to dry. Cell pellets were resuspended in PBS and kept on ice to inhibit DNA repair. Cell suspensions were rapidly mixed with LMP agarose at 0.5% kept at 37 °C and an aliquot was pipetted onto agarose-covered surface of the slide. Agarose-embedded cells were lysed by submerging slides in lysis solution (30 mM EDTA, 0.1% sodium dodecyl sulphate (SDS)) and incubated at 4 °C, 1 h in the dark. After lysis, slides were washed in Tris Borate EDTA (TBE) 1X running buffer (Tris 90 mM; boric acid 90 mM; EDTA 4 mM) for 1 min. Electrophoresis was performed for 20 min in TBE 1X buffer at 1 V/cm. Slides were subsequently washed in distilled H_2O and finally dehydrated in ice-cold methanol. Nuclei were stained with GelRed (1:1000) and visualised with a fluorescence microscope (Zeiss), using a 60X objective, connected to a CCD camera for image acquisition. At least 300 comets per cell line were analysed using CometAssay IV software (Perceptive instruments) and data from tail moments processed using Prism software. Apoptotic cells (smaller Comet head and extremely larger Comet tail) were excluded from the analysis to avoid artificial enhancement of the tail moment.

REFERENCES

1. Osborn, A. J., Elledge, S. J. & Zou, L. Checking on the fork: The DNA-replication stress-response pathway. *Trends Cell Biol.* **12**, 509–516 (2002).
2. Hills, S. A. & Diffley, J. F. X. DNA Replication and Oncogene-Induced Replicative Stress. *Curr. Biol.* **24**, R435–R444 (2014).
3. Berti, M. & Vindigni, A. Replication stress: getting back on track. *Nat. Struct. Mol. Biol.* **23**, 103–9 (2016).
4. Branzei, D. & Foiani, M. The checkpoint response to replication stress. *DNA Repair (Amst).* **8**, 1038–1046 (2009).
5. Malacaria, E., Honda, M., Franchitto, A., Spies, M. & Pichierri, P. Physiological and Pathological Roles of RAD52 at DNA Replication Forks. *Cancers (Basel).* **12**, 402 (2020).
6. Cimprich, K. A. & Cortez, D. ATR: an essential regulator of genome integrity. *Nat. Rev. Mol. Cell Biol.* **9**, 616–27 (2008).
7. Quinet, A., Lemaçon, D. & Vindigni, A. Replication Fork Reversal: Players and Guardians. *Mol. Cell* **68**, 830–833 (2017).
8. Neelsen, K. J. & Lopes, M. Replication fork reversal in eukaryotes: from dead end to dynamic response. *Nat. Rev. Mol. Cell Biol.* **16**, 207–20 (2015).
9. San Filippo, J., Sung, P. & Klein, H. Mechanism of eukaryotic homologous recombination. *Annu. Rev. Biochem.* **77**, 229–57 (2008).
10. Lord, C. J. & Ashworth, A. BRCAness revisited. *Nat. Rev. Cancer* **16**, 110–120 (2016).
11. Tutt, A. & Ashworth, A. The relationship between the roles of BRCA genes in DNA repair and cancer predisposition. *Trends Mol. Med.* **8**, 571–6 (2002).
12. Schlacher, K. *et al.* Double-Strand Break Repair-Independent Role for BRCA2 in Blocking Stalled Replication Fork Degradation by MRE11. *Cell* **145**, 529–542 (2011).
13. Lemaçon, D. *et al.* MRE11 and EXO1 nucleases degrade reversed forks and elicit MUS81-dependent fork rescue in BRCA2-deficient cells. *Nat. Commun.* **8**, 860 (2017).
14. Mijic, S. *et al.* Replication fork reversal triggers fork degradation in BRCA2-defective cells. *Nat. Commun.* **8**, 859 (2017).
15. Chaudhuri, A. R. *et al.* Replication fork stability confers chemoresistance in BRCA-deficient cells. *Nature* **535**, 382–7 (2016).
16. Rondinelli, B. *et al.* EZH2 promotes degradation of stalled replication forks by recruiting MUS81 through histone H3 trimethylation. *Nat. Cell Biol.* **19**, 1371–1378 (2017).
17. Dungrawala, H. *et al.* RADX Promotes Genome Stability and Modulates Chemosensitivity

by Regulating RAD51 at Replication Forks. *Mol. Cell* **67**, 374-386.e5 (2017).

18. Lai, X. *et al.* MUS81 nuclease activity is essential for replication stress tolerance and chromosome segregation in BRCA2-deficient cells. *Nat. Commun.* **8**, 15983 (2017).
19. Pepe, A. & West, S. C. MUS81-EME2 promotes replication fork restart. *Cell Rep.* **7**, 1048–1055 (2014).
20. Wild, P. & Matos, J. Cell cycle control of DNA joint molecule resolution. *Curr. Opin. Cell Biol.* **40**, 74–80 (2016).
21. Palma, A. *et al.* Phosphorylation by CK2 regulates MUS81/EME1 in mitosis and after replication stress. *Nucleic Acids Res.* **46**, 5109–5124 (2018).
22. Giaccherini, C., Scaglione, S., Coulon, S., Dehé, P.-M. & Gaillard, P.-H. L. Regulation of Mus81-Eme1 structure-specific endonuclease by Eme1 SUMO-binding and Rad3ATR kinase is essential in the absence of Rqh1BLM helicase. *PLoS Genet.* **18**, e1010165 (2022).
23. Boddy, M. N. *et al.* Damage tolerance protein Mus81 associates with the FHA1 domain of checkpoint kinase Cds1. *Mol. Cell. Biol.* **20**, 8758–8766 (2000).
24. Kai, M., Boddy, M. N., Russell, P. & Wang, T. S. F. Replication checkpoint kinase Cds1 regulates Mus81 to preserve genome integrity during replication stress. *Genes Dev.* **19**, 919–932 (2005).
25. Dehé, P.-M. *et al.* Regulation of Mus81-Eme1 Holliday junction resolvase in response to DNA damage. *Nat. Struct. Mol. Biol.* **20**, 598–603 (2013).
26. Ciccia, A. & Elledge, S. J. The DNA Damage Response: Making It Safe to Play with Knives. *Mol. Cell* **40**, 179–204 (2010).
27. Matos, J. & West, S. C. Holliday junction resolution: Regulation in space and time. *DNA Repair (Amst).* **19**, 176–181 (2014).
28. Hanada, K. *et al.* The structure-specific endonuclease Mus81 contributes to replication restart by generating double-strand DNA breaks. *Nat. Struct. Mol. Biol.* **14**, 1096–1104 (2007).
29. Franchitto, A. *et al.* Replication fork stalling in WRN-deficient cells is overcome by prompt activation of a MUS81-dependent pathway. *J. Cell Biol.* **183**, 241–252 (2008).
30. Técher, H. *et al.* Signaling from Mus81-Eme2-Dependent DNA Damage Elicited by Chk1 Deficiency Modulates Replication Fork Speed and Origin Usage. *Cell Rep.* 1–14 (2016) doi:10.1016/j.celrep.2015.12.093.
31. Bell, D. W. *et al.* Heterozygous germ line hCHK2 mutations in Li-Fraumeni syndrome. *Science* **286**, 2528–31 (1999).
32. Li, J. *et al.* Structural and functional versatility of the FHA domain in DNA-damage signaling by the tumor suppressor kinase Chk2. *Mol. Cell* **9**, 1045–1054 (2002).

33. Murfuni, I. *et al.* The WRN and MUS81 proteins limit cell death and genome instability following oncogene activation. *Oncogene* **32**, 610–20 (2012).

34. Murfuni, I. *et al.* Survival of the Replication Checkpoint Deficient Cells Requires MUS81-RAD52 Function. *PLoS Genet.* **9**, e1003910 (2013).

35. Forment, J. V., Blasius, M., Guerini, I. & Jackson, S. P. Structure-specific DNA endonuclease mus81/eme1 generates DNA damage caused by chk1 inactivation. *PLoS One* **6**, e23517 (2011).

36. Rickman, K. & Smogorzewska, A. Advances in understanding DNA processing and protection at stalled replication forks. *J. Cell Biol.* **218**, 1096–1107 (2019).

37. Berti, M. *et al.* Human RECQ1 promotes restart of replication forks reversed by DNA topoisomerase I inhibition. *Nat. Struct. Mol. Biol.* **20**, 347–54 (2013).

38. Hengel, S. R. *et al.* Small-molecule inhibitors identify the RAD52-ssDNA interaction as critical for recovery from replication stress and for survival of BRCA2 deficient cells. *Elife* **5**, (2016).

39. Malacaria, E. *et al.* Rad52 prevents excessive replication fork reversal and protects from nascent strand degradation. *Nat. Commun.* **10**, 1–19 (2019).

40. Iannascoli, C., Palermo, V., Murfuni, I., Franchitto, A. & Pichierri, P. The WRN exonuclease domain protects nascent strands from pathological MRE11/EXO1-dependent degradation. *Nucleic Acids Res.* **43**, 9788–803 (2015).

41. Kolinjivadi, A. M. *et al.* Smarcal1-Mediated Fork Reversal Triggers Mre11-Dependent Degradation of Nascent DNA in the Absence of Brca2 and Stable Rad51 Nucleofilaments. *Mol. Cell* **67**, 867-881.e7 (2017).

42. Durocher, D. *et al.* The molecular basis of FHA domain:phosphopeptide binding specificity and implications for phospho-dependent signaling mechanisms. *Mol. Cell* **6**, 1169–1182 (2000).

43. Nair, N., Castor, D., Macartney, T. & Rouse, J. Identification and characterization of MUS81 point mutations that abolish interaction with the SLX4 scaffold protein. *DNA Repair (Amst).* **24**, 131–137 (2014).

44. Wyatt, H. D. M., Laister, R. C., Martin, S. R., Arrowsmith, C. H. & West, S. C. The SMX DNA Repair Tri-nuclease. *Mol. Cell* **65**, 848-860.e11 (2017).

45. Francesca Blandino, Eva Malacaria, Giusj Monia Pugliese, Annapaola Franchitto, P. P. PHOSPHORYLATION STATUS OF MUS81 IS A MODIFIER OF OLAPARIB SENSITIVITY IN BRCA2-DEFICIENT CELLS. *bioRxiv* (2022) doi:10.1101/2022.08.13.503764.

46. Lambert, S. *et al.* Homologous recombination restarts blocked replication forks at the expense of genome rearrangements by template exchange. *Mol. Cell* **39**, 346–359 (2010).
47. Doe, C. L., Ahn, J. S., Dixon, J. & Whitby, M. C. Mus81-Eme1 and Rqh1 involvement in processing stalled and collapsed replication forks. *J. Biol. Chem.* **277**, 32753–32759 (2002).
48. Duda, H. *et al.* A Mechanism for Controlled Breakage of Under-replicated Chromosomes during Mitosis. *Dev. Cell* **39**, 740–755 (2016).
49. Pepe, A. & West, S. C. Substrate specificity of the MUS81-EME2 structure selective endonuclease. *Nucleic Acids Res.* **42**, 3833–3845 (2014).
50. Couch, F. B. *et al.* ATR phosphorylates SMARCAL1 to prevent replication fork collapse. *Genes Dev.* **27**, 1610–1623 (2013).
51. Almawi, A. W., Matthews, L. A. & Guarné, A. FHA domains: Phosphopeptide binding and beyond. *Prog. Biophys. Mol. Biol.* **127**, 105–110 (2017).
52. Matthews, L. A. *et al.* A novel non-canonical forkhead-associated (FHA) domain-binding interface mediates the interaction between Rad53 and Dbf4 proteins. *J. Biol. Chem.* **289**, 2589–99 (2014).
53. Dhoonmoon, A., Nicolae, C. M. & Moldovan, G.-L. The KU-PARP14 axis differentially regulates DNA resection at stalled replication forks by MRE11 and EXO1. *Nat. Commun.* **13**, 5063 (2022).
54. Lv, J., Qian, Y., Ni, X., Xu, X. & Dong, X. Feedback regulation of methyl methanesulfonate and ultraviolet-sensitive gene clone 81 via ATM/Chk2 pathway contributes to the resistance of MCF-7 breast cancer cells to cisplatin. *Tumour Biol.* **39**, 1010428317694307 (2017).
55. Sancar, A., Lindsey-Boltz, L. a, Unsal-Kaçmaz, K. & Linn, S. Molecular mechanisms of mammalian DNA repair and the DNA damage checkpoints. *Annu. Rev. Biochem.* **73**, 39–85 (2004).
56. Apostolou, P. & Papasotiriou, I. Current perspectives on CHEK2 mutations in breast cancer. *Breast cancer (Dove Med. Press.* **9**, 331–335 (2017).
57. Hua, Z. *et al.* Crystal structure of the human MUS81-EME2 complex. *Structure* **30**, 743-752.e3 (2022).
58. Stolarova, L. *et al.* CHEK2 Germline Variants in Cancer Predisposition: Stalemate Rather than Checkmate. *Cells* **9**, (2020).
59. Boonen, R. A. C. M. *et al.* Functional Analysis Identifies Damaging CHEK2 Missense Variants Associated with Increased Cancer Risk. *Cancer Res.* **82**, 615–631 (2022).
60. Xue, Y. *et al.* GPS 2.0, a tool to predict kinase-specific phosphorylation sites in hierarchy. *Mol. Cell. Proteomics* **7**, 1598–608 (2008).

61. Pichierri, P., Nicolai, S., Cignolo, L., Bignami, M. & Franchitto, a. The RAD9–RAD1–HUS1 (9.1.1) complex interacts with WRN and is crucial to regulate its response to replication fork stalling. *Oncogene* **31**, 2809–2823 (2012).

LEGENDS TO FIGURES

Figure 1. CHK2 form a complex with MUS81 that is stimulated upon replication stress and support MUS81-dependent DSB formation. A) HEK293T cells were transfected as indicated and 48h after treated with HU 2mM or nocodazole for 24h. After lysis, CHK2 or MUS81 were immunoprecipitated using anti-HA or GFP as indicated. The numbers below the IP represent quantification in arbitrary units of amount of MUS81 or CHK2 coimmunoprecipitating normalised on the fraction of CHK2 or MUS81 respectively. B). Endogenous MUS81 and CHK2 form a complex. MRC5 shMUS81 cells stably complemented with Flag-MUS81 were used to immunoprecipitate MUS81 in cells treated with HU or accumulated in mitosis with nocodazole. The numbers below the IP represent quantification in arbitrary units of amount of CHK2 coimmunoprecipitating normalised on the fraction of MUS81. C) MRC5 shMUS81 cells stably complemented with Flag-MUS81 were treated as indicated and analysed for the interaction between MUS81 and CHK2 using in situ PLA. Images show representative fields and the inset shows the mean number of spots. The graph shows the number of PLA-positive nuclei (mean±SE; n=2. * = $p < 0,5$ ANOVA). D) MRC5 shMUS81 cells stably complemented or not with Flag-MUS81 were treated as indicated and subjected to neutral Comet assay to evaluate formation of MUS81-dependent DSBs. The panel shows representative images of comet tails for each condition. Quantification of Tail moment is reported in the graph. (ns = not significant; **** = $p < 0,0001$, Student's t-test)

Figure 2. Functional interaction of CHK2 with MUS81 involves the FHA domain and is disabled by the I157T mutation. A) The wild-type and I157T-mutated GST-fused FHA fragment of CHK2 was purified from bacteria and used as bait to pull-down MUS81 from HEK293T nuclear extracts. B) MRC5 shMUS81 cells stably complemented or not with Flag-MUS81 were transiently transfected with the indicated HA-CHK2 construct and used to immunoprecipitate CHK2 in cells treated with HU. Representative immunoblots are shown. C) MRC5 shMUS81 cells stably complemented with Flag-MUS81 were transfected with the indicated HA-CHK2 construct and analysed for the interaction between MUS81 and CHK2 by anti-HA co-immunoprecipitation. D) MRC5 shMUS81 cells stably complemented or not with Flag-MUS81 were transiently transfected with the indicated CHK2 construct, treated with HU, and subjected to neutral Comet assay to evaluate formation of MUS81-dependent DSBs. Quantification of Tail moment is reported in the graph. (ns = not significant; **** = $p < 0,0001$, Student's t-test)

Figure 3. Activity of CHK2 and its interaction with MUS81 drives formation of DSBs at stalled forks in BRCA2-deficient cells. A) WB showing depletion of BRCA2 and expression of I157T-mutated CHK2 in MRC5 shMUS81 cells stably complemented with Flag-MUS81. B) MRC5 shMUS81 cells stably complemented with Flag-MUS81 were transfected with the indicated HA-CHK2 construct or treated with the BML-277 CHK2 inhibitor (CHK2i) prior to be exposed to HU 2mM and analysed for the presence of MUS81-dependent DSBs by neutral Comet assay. (**** = p<0.001, Student's t-test). Representative images are shown. C) Analysis of fork recruitment of active ATM in BRCA2-depleted cells. Doxycycline-inducible shBRCA2 MRC5 cells were depleted of BRCA2 by treatment with dox, as indicated, and treated with HU for different time-points. Recruitment of active ATM at nascent DNA at fork was analysed by SIRF using anti-pS1981ATM antibody. (*** = p<0.01; **** = p<0.001, ANOVA). Representative of PLA images are shown.

Figure 4. Interaction between MUS81 and CHK2 is dependent on fork reversal and processing. A-B) Cells were transfected with scrambled siRNA (siCTRL) or siRNA directed against BRCA2 alone or in combination with siRNA against SMARCAL1 and treated with HU prior to the evaluation of MUS81-CHK2 interaction in situ by PLA. The graphs show the number of PLA spots for each condition (n=2, * = P < 0.5; **** = P < 0.0001; Mann–Whitney test). Representative images are shown. C) Cells were depleted of BRCA2 by transfection with siRNAs and pre-treated with Olaparib before being challenged with HU as indicated. Interation between MUS81 and CHK2 was evaluated by in situ PLA. The graph shows the number of PLA spotes for each condition (n=2, **** = P < 0.0001; Mann–Whitney test). Representative images are shown. D) Cells were transfected with scrambled siRNA (siCTRL) or siRNA directed against BRCA2. Cell lysates were subjected to immunoblotting with indicated antibodies. Lamin B1 was used as loading control. Single-cell analysis of CHK2-MUS81 interaction by in situ PLA. Cells were treated as indicated in the graph. Graph shows the number of PLA spots per cell. (n=2, **** = P < 0.0001; Mann–Whitney test). Representative images are shown.

Figure 5. Activity of CHK2 and its interaction with MUS81 is required for fork restart and fork processing in BRCA2-deficient cells. A) WB showing depletion of BRCA2 and expression levels of mutant CHK2 in MRC5 shMUS81 cells stably complemented with Flag-MUS81. B) Analysis of replication fork restart using DNA fibre assay. Cells were treated as indicated in the scheme on the top. The graph shown the percentage of stalled forks for each condition. (** = P < 0.01; *** = p<0.001, ANOVA test). C) Cartoon exemplifying the use of RuvA as proxy for the presence of 4-way junctions and expected results if MUS81 is cleaving or not reversed forks. D)

Dox-regulated shBRCA2 MRC5 cells were transfected with plasmids expressing GFP-RuvA and the indicated HA-CHK2 construct. After 48h, cells were treated with HU and analysed for the presence of RuvA in chromatin by WB of chromatin fractions with the indicated antibodies. RuvA was detected using anti-GFP while CHK2 using anti-HA antibodies. Input shows expression levels of RuvA and CHK2 or MUS81 depletion. The graph shows the normalized amount of RuvA in chromatin for each condition. In blue, are highlighted conditions in which MUS81 is not working or absent. Values are presented as means ± S.E. (n=2, not significant pairs are not labelled; *=p<0.5; **=p<0.1; ANOVA)

Figure 6. Abrogation of phosphorylation of MUS81 at CHK2 sites impairs the function of MUS81 after replication stress. A) Scheme outlining the identification of *in vitro* MUS81 phosphosites. GST-fused N-terminal MUS81 fragment was incubated with recombinant CHK2 and subjected to MS/MS analyses to identify phosphopeptides and residues. B) MRC5 shMUS81 cells were transfected with plasmids expressing different MUS81 phosphomutants for each CHK2 site identified by MS. After 48h, cells were treated as indicated. Formation of DSBs was analysed by neutral Comet assay. The graph shows the mean Tail moment ± S.E. for each condition. (ns = not significant; *** = p<0.01; **** = p<0.001 Student's t-test). C) WB showing BRCA2 levels in MRC5 shMUS81 cells transiently transfected with the indicated MUS81 mutant and BRCA2 siRNAs. The graph shows the mean Tail moment ± S.E. for each condition. (ns = not significant; **** = p<0.001 Student's t-test). Representative images are shown. D) Analysis of replication fork restart using DNA fibre assay. Cells were treated as indicated in the scheme on the top. The graph shown the percentage of stalled forks for each condition. Inducible shBRCA2 MUS81 knockout MRC5cells were transfected with MUS81 WT or MUS81 97A . Cell lysates were subjected to immunoblotting with indicated antibodies. Lamin B1 (LAMIN) was used as loading control. Representative images of DNA fibres fields are presented. (**P < 0.01; ANOVA). E) Analysis of IdU tract length of restarted forks. Length of the green tracks was measured in 200 individual forks. Mean values ± SE are represented as horizontal black lines. (ns = not significant; **** P < 0.0001; Mann–Whitney test)

Figure 7. The absence of MUS81 or inability to form the CHK2-MUS81 complex similarly affects HU sensitivity of BRCA2-depleted cells. A) The wild-type or FHA mutant form of CHK2 was transiently expressed in BRCA2-depleted MRC5 cells wild-type or KO for MUS81. Viability was assessed by MTT assay after treatment with HU for 4 days. Each point represents the average number of counts from four independent experiments. B) Model of CHK2-MUS81 complex function in normal or BRCA2-depleted cells. See discussion for details.

TABLES

Table 1. Phosphorylation sites identified in the N-terminal MUS81 region by in vitro CHK2 kinase assay

Residue position	**Residue type**	**Phosphopeptide Sequence**	**Mascot score**	**m/z (charge)**	**Fragmentation type**	**Retention time**
97	Ser	TSGGDHAPDSP**Sp**GENSPAPQGR	107	734.31 (3+)	ETD	14.4 min
86	Thr	HR**Tp**SGGDHAPDSPSGENSPAPQGR	52	832.04 (3+)	CID	13.9 min

a

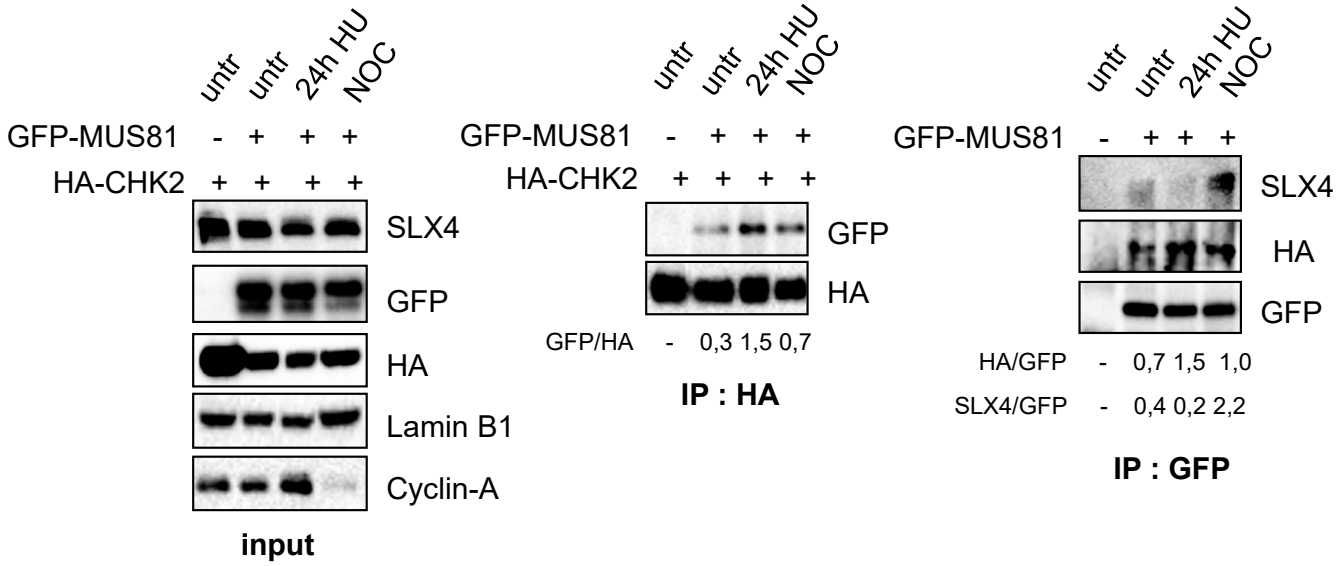

b

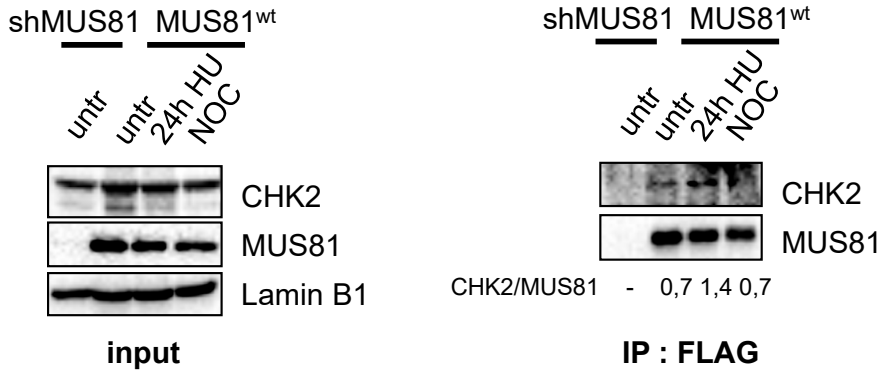

PLA (FLAG)MUS81-CHK2

c

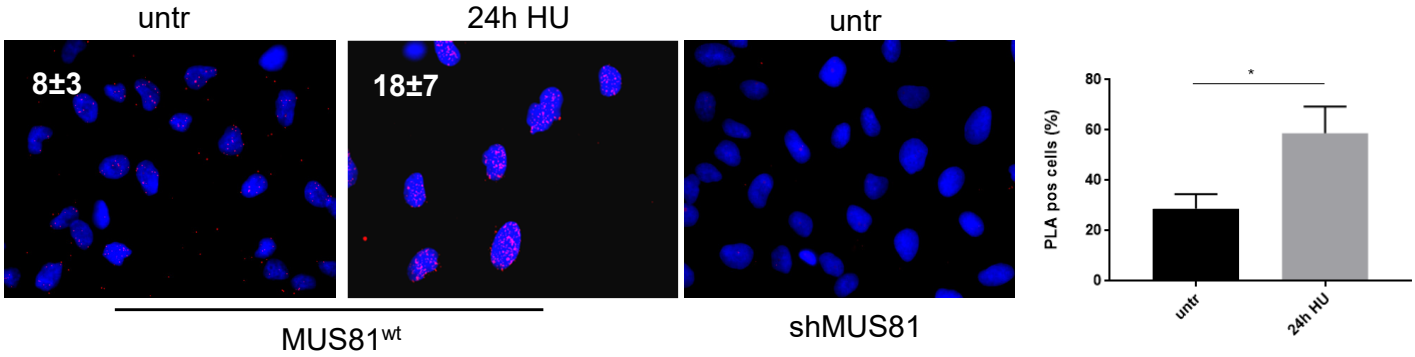

d

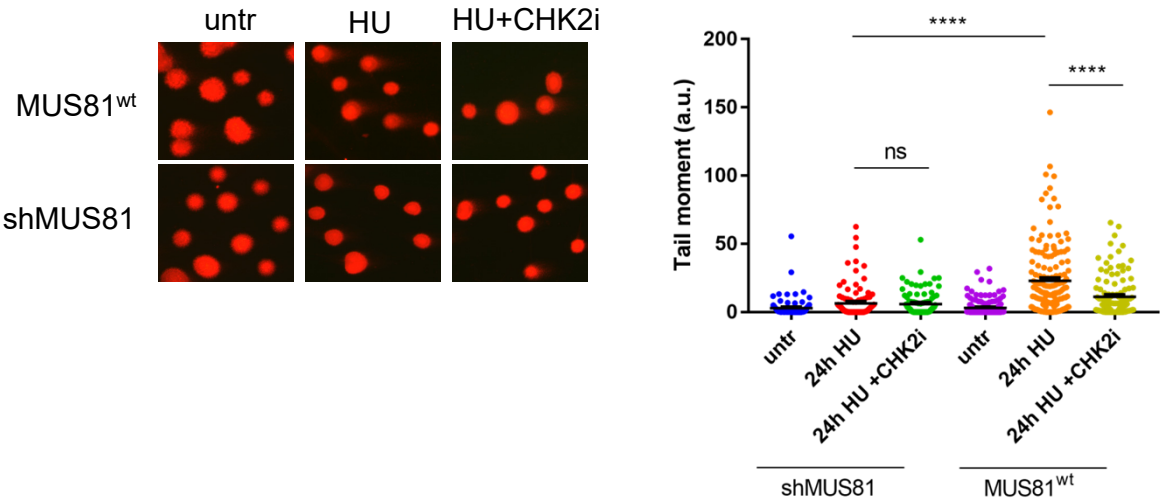

Figure 1

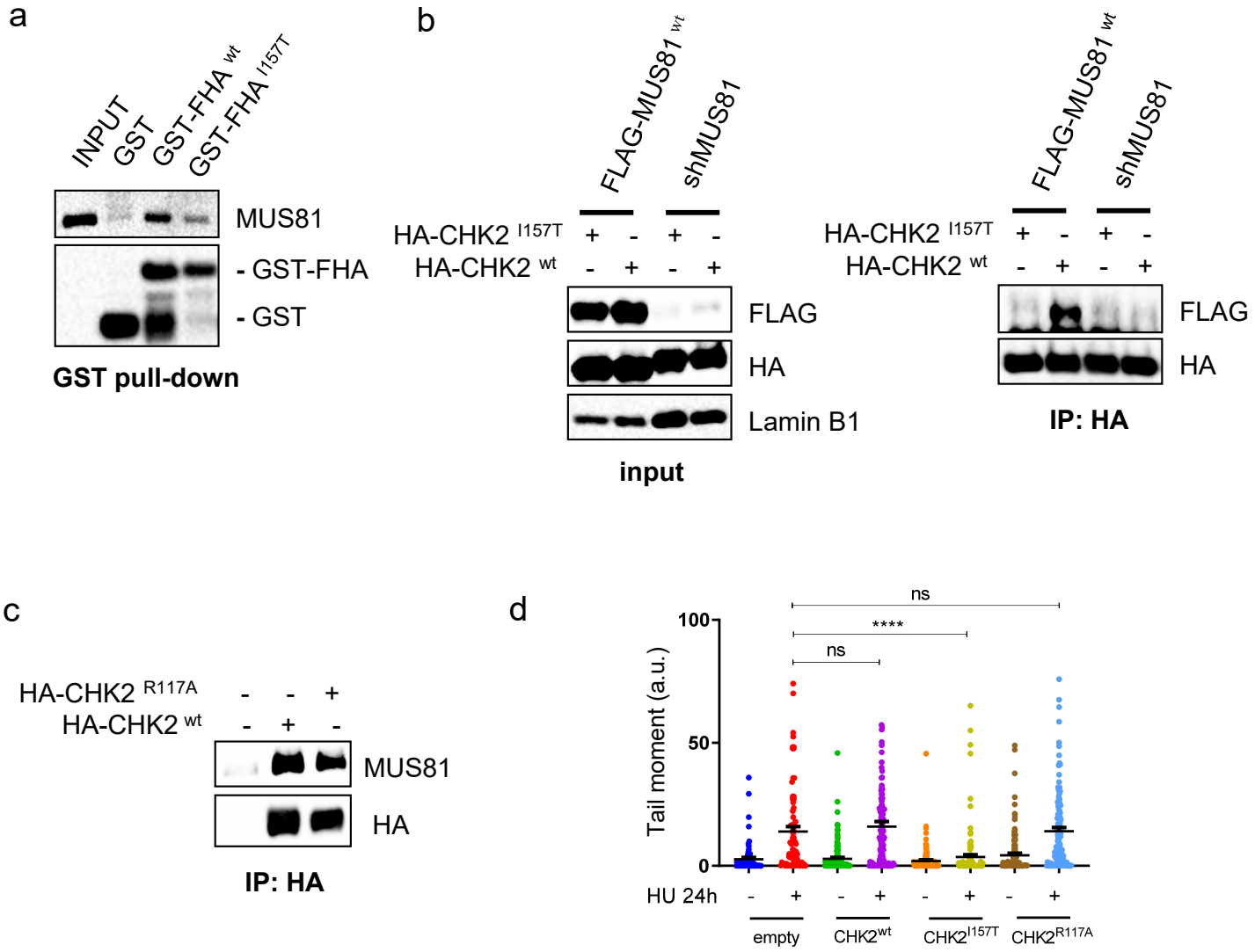
a
INPUT
GST
GST-FHA wt
GST-FHA I157T
MUS81
- GST-FHA
- GST
GST pull-down
b
FLAG-MUS81 wt
shMUS81
HA-CHK2 I157T + - + -
HA-CHK2 wt - + - +
FLAG
HA
Lamin B1
input
FLAG-MUS81 wt
shMUS81
HA-CHK2 I157T + - + -
HA-CHK2 wt - + - +
FLAG
HA
IP: HA
c
HA-CHK2 R117A - - +
HA-CHK2 wt - + -
MUS81
HA
IP: HA
d
ns
****
ns
100
50
0
Tail moment (a.u.)
HU 24h - + - + - + - +
empty
CHK2wt
CHK2I157T
CHK2R117A

Figure 2

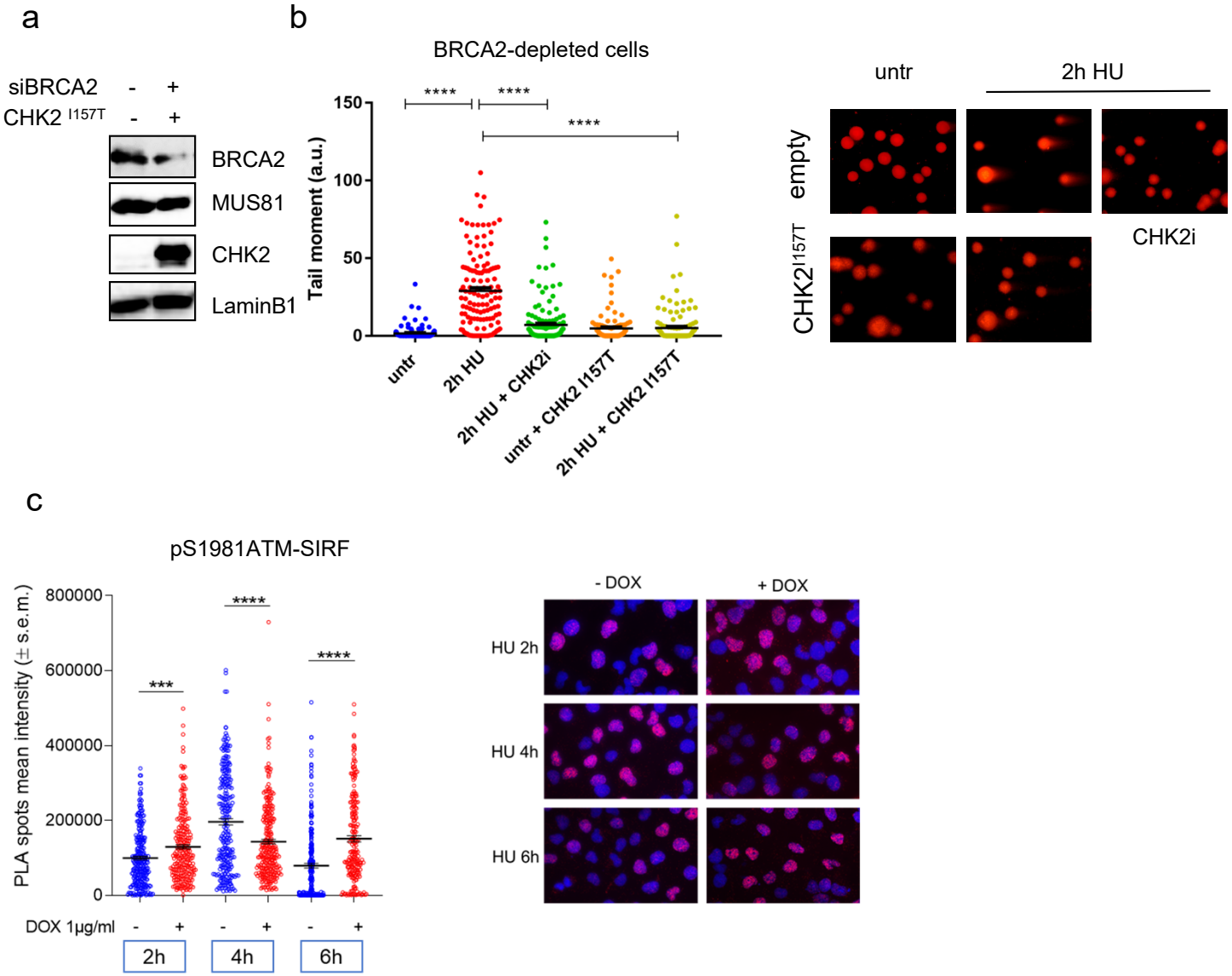
a
siBRCA2 - +
CHK2 I157T - +
BRCA2
MUS81
CHK2
LaminB1
b
BRCA2-depleted cells
Tail moment (a.u.)
150
100
50
0
****
****
****
untr
2h HU
2h HU + CHK2i
untr + CHK2 I157T
2h HU + CHK2 I157T
untr
2h HU
empty
CHK2I157T
CHK2i
c
pS1981ATM-SIRF
PLA spots mean intensity (± s.e.m.)
800000
600000
400000
200000
0
***
****
****
DOX 1µg/ml - + - + - +
2h
4h
6h
- DOX
+ DOX
HU 2h
HU 4h
HU 6h

Figure 3

a

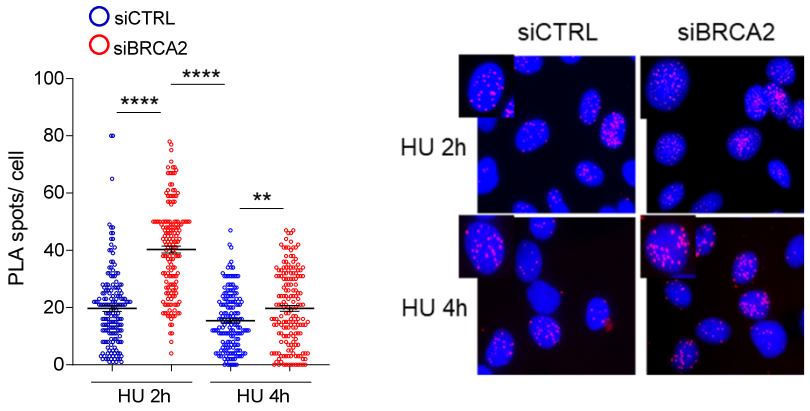

b

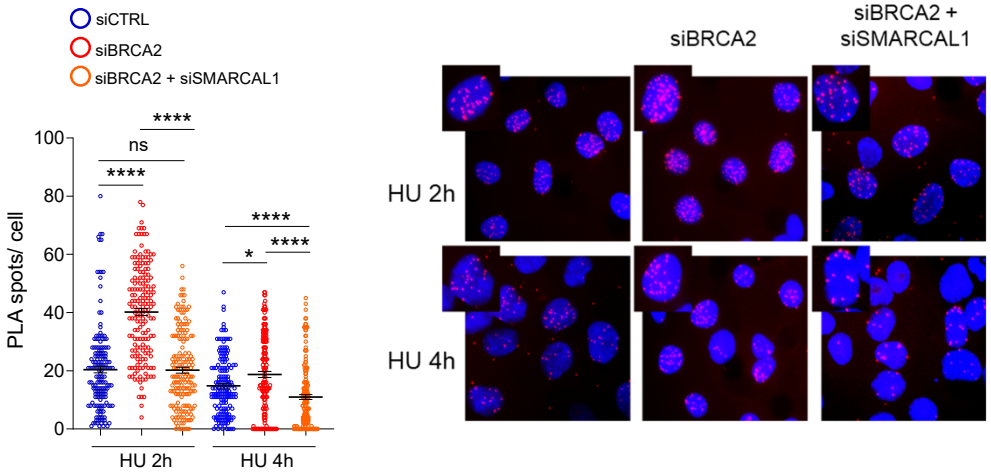

c

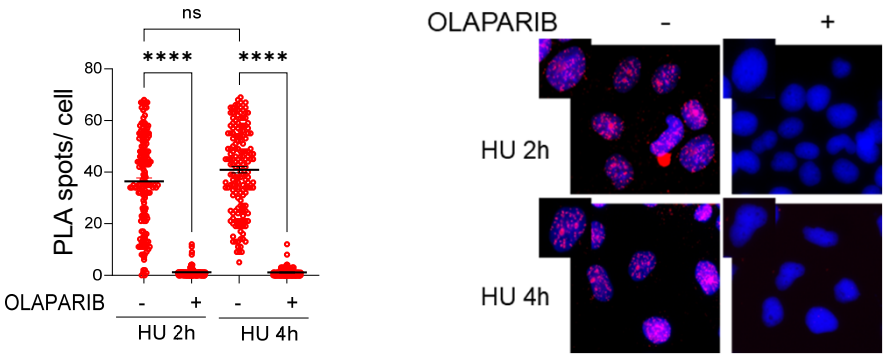

d

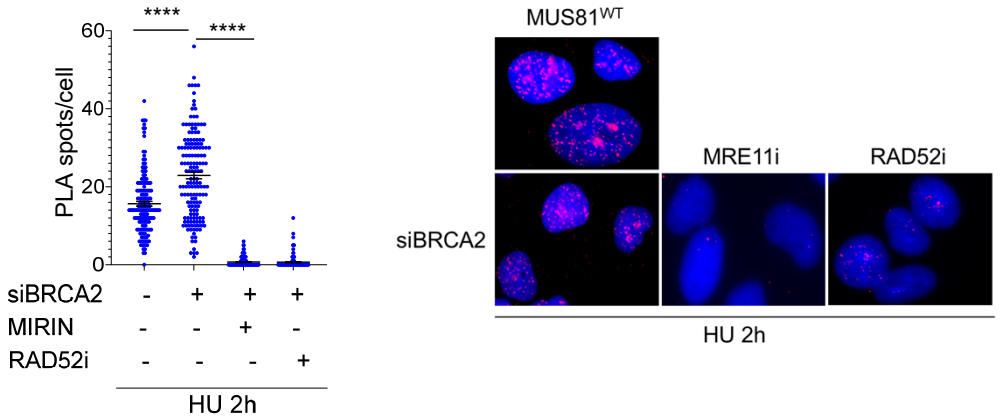

Figure 4

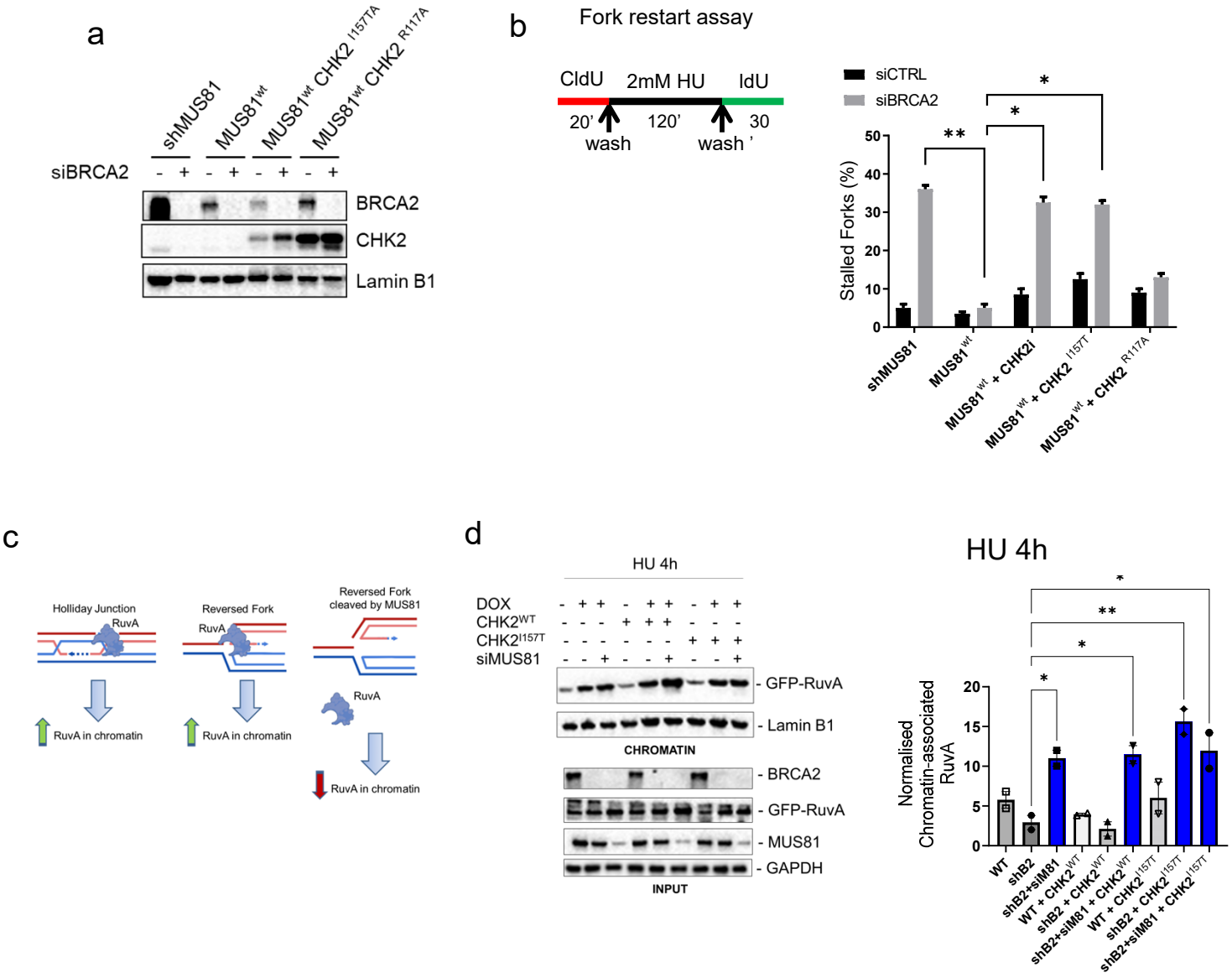
a
shMUS81
MUS81wt
MUS81wt CHK2 I157TA
MUS81wt CHK2 R117A
siBRCA2
- + - + - + - +
BRCA2
CHK2
Lamin B1
b
Fork restart assay
CldU
2mM HU
IdU
20'
120'
30
wash
wash '
siCTRL
siBRCA2
Stalled Forks (%)
shMUS81
MUS81wt
MUS81wt + CHK2i
MUS81wt + CHK2 I157T
MUS81wt + CHK2 R117A
c
Holliday Junction
RuvA
RuvA in chromatin
Reversed Fork
Reversed Fork cleaved by MUS81
d
HU 4h
DOX
CHK2WT
CHK2I157T
siMUS81
GFP-RuvA
Lamin B1
CHROMATIN
BRCA2
GFP-RuvA
MUS81
GAPDH
INPUT
HU 4h
Normalised Chromatin-associated RuvA
WT
shB2
shB2+siM81
WT + CHK2WT
shB2 + CHK2WT
shB2+siM81 + CHK2WT
WT + CHK2I157T
shB2 + CHK2I157T
shB2+siM81 + CHK2I157T

Figure 5

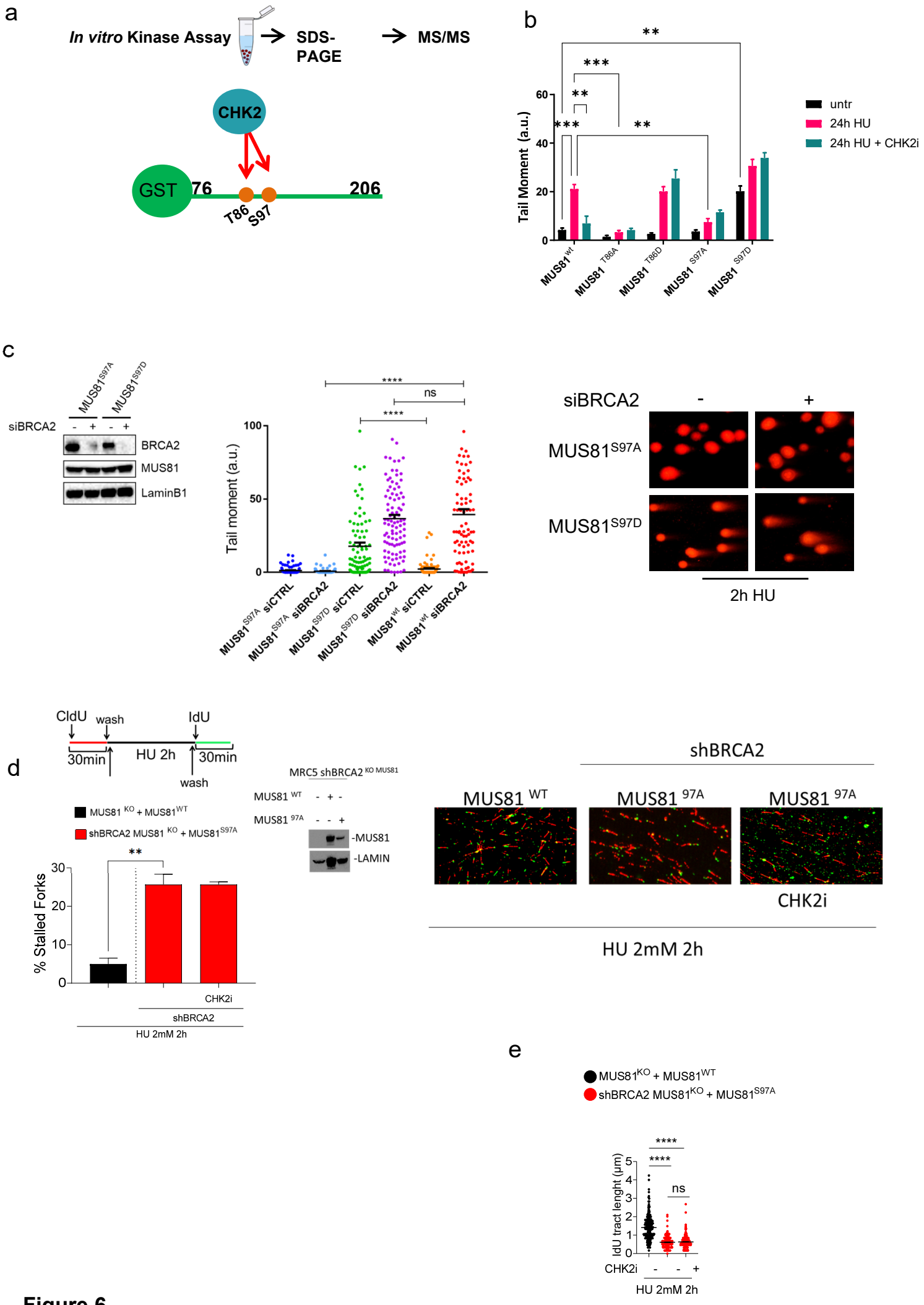
a
In vitro Kinase Assay
SDS-PAGE
MS/MS
CHK2
GST
76
206
T86
S97
b
Tail Moment (a.u.)
untr
24h HU
24h HU + CHK2i
MUS81 wt
MUS81 T86A
MUS81 T86D
MUS81 S97A
MUS81 S97D
c
siBRCA2
BRCA2
MUS81
LaminB1
Tail moment (a.u.)
ns
siBRCA2
MUS81 S97A
MUS81 S97D
2h HU
d
CldU
wash
IdU
30min
HU 2h
30min
wash
MUS81 KO + MUS81 WT
shBRCA2 MUS81 KO + MUS81 S97A
% Stalled Forks
CHK2i
shBRCA2
HU 2mM 2h
MRC5 shBRCA2 KO MUS81
MUS81 WT
MUS81 97A
-MUS81
-LAMIN
shBRCA2
MUS81 WT
MUS81 97A
MUS81 97A
CHK2i
HU 2mM 2h
e
MUS81KO + MUS81WT
shBRCA2 MUS81KO + MUS81S97A
IdU tract lenght (µm)
ns
CHK2i
HU 2mM 2h

Figure 6

a

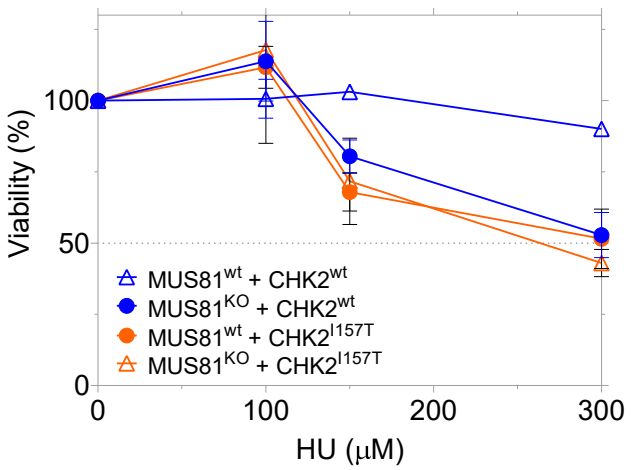
Viability (%)
100
50
0
0
100
200
300
HU (μM)
MUS81wt + CHK2wt
MUS81KO + CHK2wt
MUS81wt + CHK2I157T
MUS81KO + CHK2I157T

b

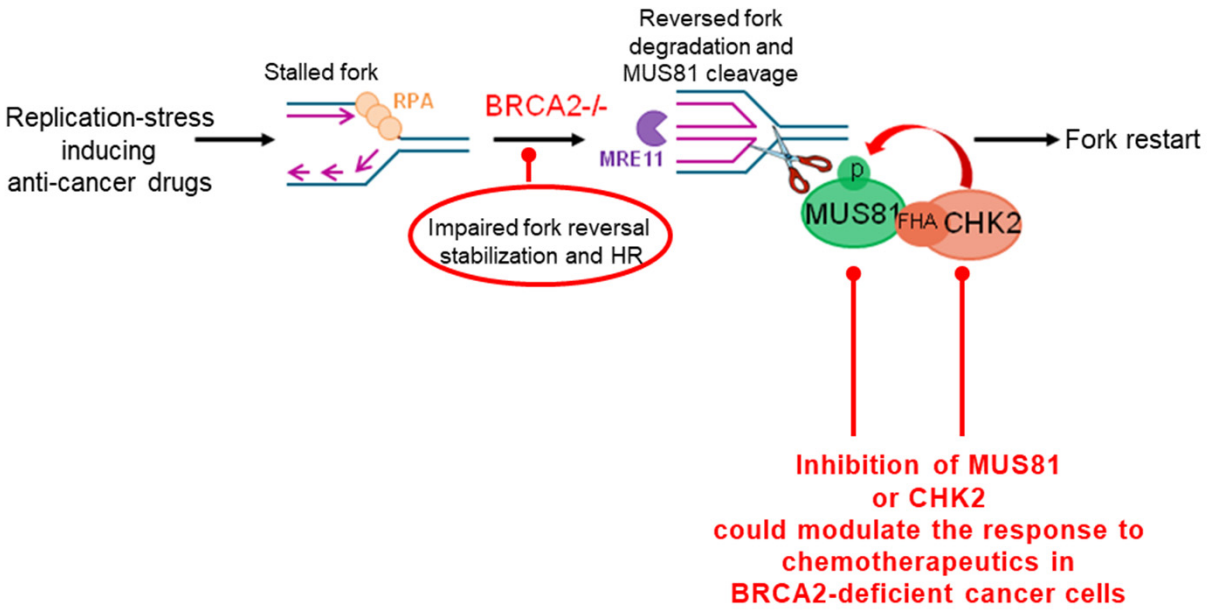
Replication-stress inducing anti-cancer drugs
Stalled fork
RPA
BRCA2-/-
Impaired fork reversal stabilization and HR
Reversed fork degradation and MUS81 cleavage
MRE11
p
MUS81
FHA
CHK2
Fork restart
Inhibition of MUS81 or CHK2 could modulate the response to chemotherapeutics in BRCA2-deficient cancer cells

Figure 7